

Quantum Fisher information of entangled coherent state in the presence of photon losses: exact solution

Y. M. Zhang, X. W. Li,¹ W. Yang,^{2,*} and G. R. Jin^{1,†}

¹*Department of Physics, Beijing Jiaotong University, Beijing 100044, China*

²*Beijing Computational Science Research Center, Beijing 100084, China*

(Dated: July 30, 2013)

We investigate the performance of entangled coherent state for quantum enhanced phase estimation. An exact analytical expression of quantum Fisher information is derived to show the role of photon losses on the ultimate phase sensitivity. We find a transition of the sensitivity from the Heisenberg scaling to the classical scaling due to quantum decoherence of the photon state. This quantum-classical transition is uniquely determined by the number of photons being lost, instead of the number of incident photons or the photon loss rate alone. Our results also reveal that a crossover of the sensitivity between the entangled coherent state and the NOON state can occur even for very small photon loss rate.

PACS numbers: 42.50.Dv, 42.50.Lc, 03.65.Ta, 06.20.Dk

I. INTRODUCTION

The estimation of parameters characterizing dynamical processes is essential to science and technology. A typical parameter estimation consists of three steps. Firstly, the input state $|\psi_{\text{in}}\rangle$ of the sensor is prepared. Secondly, the sensor undergoes the ϕ -dependent dynamical process $\hat{U}(\phi)$ and evolve to the output state $|\psi\rangle$. Finally, a measurement is made on the output state and the outcome x is used by suitable data processing to produce an unbiased estimator $\hat{\phi}(x)$ of the parameter ϕ . The precision of the estimation is quantified by the standard deviation $\delta\phi = \langle(\hat{\phi}(x) - \phi)^2\rangle$, which is determined by the input state $|\psi_{\text{in}}\rangle$ [1–7], the nature of the dynamical process $\hat{U}(\phi)$ [8–13], the observable being measured [14–18], and the specific data processing technique. The precision of the estimator $\hat{\phi}_{\text{opt}}(x)$ from optimal data processing is limited by the Cramér-Rao inequality [19, 20] as $\delta\phi_{\text{opt}} \geq 1/\sqrt{F(\phi)}$, where $F(\phi)$ is the classical Fisher information, determined by $|\psi_{\text{in}}\rangle$, $\hat{U}(\phi)$, and the measurement scheme. Given $|\psi_{\text{in}}\rangle$ and $\hat{U}(\phi)$, maximizing $F(\phi)$ over all possible measurements gives the quantum Fisher information (QFI) F_Q and hence the quantum Cramér-Rao bound $\delta\phi_{\text{min}} = 1/\sqrt{F_Q}$ [21–26] on the attainable precision to estimate the phase ϕ .

In general, the best precision $\delta\phi_{\text{min}}$ improves with increasing amount of resources N employed in the measurement, e.g., the number of photons in optical phase estimation or the total duration of measurements in high-precision magnetic field or electric field sensing. For separable input states, the QFI $F_Q \sim N$ gives the classical limit $\delta\phi_{\text{min}} \sim 1/\sqrt{N}$, in agreement with classical central limit theorem. To obtain an enhanced precision, it is necessary to utilize quantum resources such as coherence, entanglement, and squeezing in the input state for maximizing the QFI and hence the precision. This is a central issue in quantum metrology [27–30]. In the absence of noise, it has been well established that by utilizing quantum

entanglement, the QFI can be enhanced up to $F_Q \sim N^2$ and hence the precision $\delta\phi_{\text{min}} \sim 1/N$, beating the Heisenberg limit [4–7, 31–34]. This limit is ultimate estimation precision allowed by quantum resource with definite particle number. In the presence of noises, however, it is not clear whether the Heisenberg limit can still be achieved [35–37], and whether entanglement is still a useful resource for quantum metrology.

A paradigmatic example is the estimation of relative phase shift between the two modes propagating on different arms of the Mach-Zehnder interferometer (MZI). Precise phase estimation is important for multiple areas of scientific research [17], such as imaging, sensing, and information processing. In the absence of noise, the classical limit $\delta\phi_{\text{min}} \sim 1/\sqrt{\bar{n}}$ (\bar{n} is the average number of photons) for classical coherent state can be dramatically improved by using nonclassical states of the light. The maximally entangled NOON states $\sim |N, 0\rangle_{1,2} + |0, N\rangle_{1,2}$ (also called the GHZ state in atomic spectroscopy) has been prepared in experiments for pursuing the Heisenberg-limited phase estimation [4–6]. However, the NOON states are extremely fragile to photon losses [35–44]. In a lossy interferometer, it has been shown that a transition of the precision from the Heisenberg limit to the shot-noise limit can occur with the increase of particle number N [36, 37].

Recently, a specific coherent superposition of the NOON states, the entangled coherent state (ECS) $\sim |\alpha, 0\rangle_{1,2} + |0, \alpha\rangle_{1,2}$, was proposed as the input state for enhanced precision [42]. In the absence of photon losses, the precision of the ECS can surpass that of the NOON state (i.e., the Heisenberg limit, $\delta\phi_{\text{min}} = 1/\bar{n}$). In the presence of photon losses, numerical simulation suggests that the ECS outperforms the NOON state for photon numbers $\bar{n} \lesssim 5$. For a small photon number $\bar{n} \sim 5$, the precision is better than the classical limit by a factor $\sqrt{\bar{n}} \sim 2$. To achieve more significant enhancement for practical applications, a much larger photon numbers are required. The performance with a large amount of resources is an important benchmark for a realistic quantum enhanced estimation scheme. Therefore, a careful analysis of the QFI and the ultimate precision for the input ECS with large \bar{n} is necessary.

In this paper, we present an exact analytical result of the

*Electronic address: wenyang@csrc.ac.cn

†Electronic address: grjin@bjtu.edu.cn

QFI for the entangled coherent state with arbitrary \bar{n} , which provides counter-intuitive physics that is inaccessible from previous numerical simulations. To understand why the ECS is better than the NOON state, we first consider an arbitrary superposition of the NOON states and find the QFI $F_Q \geq \bar{n}^2$, leading to a sub-Heisenberg limited sensitivity $\delta\phi_{\min} \leq 1/\bar{n}$. Next, we investigate the role of photon losses on the QFI and hence the ultimate precision of the ECS. An exact result of the QFI is derived, which is the sum of the classical term $\propto \bar{n}$ and the Heisenberg term $\propto \bar{n}^2$. We show that the photon losses suppresses exponentially off-diagonal (coherence) part of the reduced density matrix $\hat{\rho}$ and hence the Heisenberg term, while leaving the classical term largely unchanged. The loss-induced quantum decoherence leads to a transition of the estimation precision from the Heisenberg scaling to the classical scaling as the number of lost photons $R\bar{n}$ increases, where R is the photon loss rate and \bar{n} is the mean photon number of the initial ECS. This behavior is in sharp contrast to the NOON state, for which the photon losses eliminate completely the phase information stored in the coherence part of $\hat{\rho}$. The ultimate precision of the NOON state gets even worse than the classical limit when $R\bar{n} \gg 1$. Surprisingly, we find that the precision of the NOON state may be better than that of the ECS within the crossover region at $R\bar{n} \sim 1$. This is because although the classical term of the ECS is robust against the photon losses, the Heisenberg term decays about twice as quick as that of the NOON state.

II. SUB-HEISENBERG LIMITED PHASE SENSITIVITY WITH A SUPERPOSITION OF NOON STATES

Firstly, let us consider an *arbitrary* coherent superposition of the NOON states as the input state after the first beam splitter of a two-mode MZI,

$$|\psi_{\text{in}}\rangle = \sum_{n=0}^{\infty} c_n \frac{|n\rangle_1 + |n\rangle_2}{\sqrt{2}}, \quad (1)$$

where, for brevity, we introduce the notations $|n\rangle_1 \equiv |n\rangle_1|0\rangle_2$ and $|n\rangle_2 \equiv |0\rangle_1|n\rangle_2$, representing n photons in the mode 1 (or 2) and the other mode in vacuum. To analyze possible achievable phase sensitivity with $|\psi_{\text{in}}\rangle$, we directly evaluate the QFI of the outcome state after phase accumulation $|\psi(\phi)\rangle = \hat{U}(\phi)|\psi_{\text{in}}\rangle = e^{i\phi\hat{G}}|\psi_{\text{in}}\rangle$, where \hat{G} is the generator of phase shift. For a lossless MZI, $|\psi\rangle$ is a pure state and the QFI is given by the well-known formula [21–26]: $F_Q = 4(\langle\psi'|\psi'\rangle - |\langle\psi'|\psi\rangle|^2) = 4(\langle\hat{G}^2\rangle - \langle\hat{G}\rangle^2)$, where $|\psi'\rangle \equiv \partial|\psi\rangle/\partial\phi$ and the expectation values are taken with respect to $|\psi_{\text{in}}\rangle$. Considering a linear phase-shift generator $\hat{G} = \hat{n}_2$ [35, 42], with the photon number operators $\hat{n}_2 = \hat{a}_2^\dagger\hat{a}_2$ and $\hat{n}_1 = \hat{a}_1^\dagger\hat{a}_1$, we obtain the QFI

$$F_Q = 4(\langle\hat{n}_2^2\rangle - \langle\hat{n}_2\rangle^2) = 2\langle\hat{n}^2\rangle - \langle\hat{n}\rangle^2, \quad (2)$$

where we have used the relation $\langle\hat{n}_1^l\rangle = \langle\hat{n}_2^l\rangle = \langle\hat{n}^l\rangle/2$ (for $l = 1, 2, \dots$), which, together with $\langle\hat{n}_1\hat{n}_2\rangle = 0$ are valid for Eq. (1). Since $\langle\hat{n}^2\rangle \geq \langle\hat{n}\rangle^2$, we have $F_Q \geq \bar{n}^2$, where $\bar{n} = \langle\hat{n}\rangle$ is the mean photon number of $|\psi_{\text{in}}\rangle$. This inequality also applies

to another kind of phase-shift generator $\hat{G} = (\hat{n}_2 - \hat{n}_1)/2$, for which $F_Q = \langle\hat{n}^2\rangle$. They suggest that a sub-Heisenberg limited phase sensitivity $\delta\phi_{\min} < 1/\bar{n}$ can be achievable with an arbitrary coherent superposition of the NOON states, as Eq. (1). The equality $\delta\phi_{\min} = 1/\bar{n}$, known as the Heisenberg limit, is attained by the NOON state [4–7, 31–34] $(|N\rangle_1 + |N\rangle_2)/\sqrt{2}$ with $\bar{n} = N$.

Next, we review the recently proposed ECS state [45, 46]: $\mathcal{N}_\alpha(|\alpha\rangle_1 + |\alpha\rangle_2)$ as a special case of the superposition of NOON states, where $\mathcal{N}_\alpha = [2(1 + e^{-|\alpha|^2})]^{-1/2}$ is the normalization constant and $|\alpha\rangle_1 \equiv |\alpha\rangle_1|0\rangle_2$ denotes a coherent state in the sensor mode 1 and vacuum in the sensor mode 2 and similarly for $|\alpha\rangle_2 \equiv |\alpha\rangle_2|0\rangle_1$. The ECS can be generated by passing a coherent state $|\alpha/\sqrt{2}\rangle_1$ and a coherent state superposition $\sim |\alpha/\sqrt{2}\rangle_2 + |-\alpha/\sqrt{2}\rangle_2$ (experimentally available for $\alpha \approx 2$ [47]) through a 50:50 beam splitter [42]. In the absence of photon losses, using the ECS as the input state and considering the phase accumulation dynamics $\hat{U}(\phi) = e^{i\phi\hat{n}_2}$ [35, 42], we obtain $\bar{n} = \langle\hat{n}\rangle = 2\mathcal{N}_\alpha^2|\alpha|^2$, $\langle\hat{n}^2\rangle = 2\mathcal{N}_\alpha^2|\alpha|^2(|\alpha|^2 + 1)$, and the quantum Fisher information

$$F_Q = 2\bar{n}[1 + w(\bar{n}e^{-\bar{n}})] + \bar{n}^2, \quad (3)$$

where we have used $\bar{n} = |\alpha|^2/(1 + e^{-|\alpha|^2})$ and hence $w(\bar{n}e^{-\bar{n}}) = \bar{n}e^{-|\alpha|^2}$. Here, $w(z)$ denotes the Lambert W function (also called the product logarithm), which gives the principal solution for w in $z = we^w$. For mean photon number $\bar{n} \approx |\alpha|^2 \gg 1$, we have $w(\bar{n}e^{-\bar{n}}) \approx 0$ and $F_Q \approx \bar{n}(\bar{n} + 2)$. From Fig. 1(a), one can find that $\delta\phi_{\min}$ of the ECS (the blue solid line) is better than that of the NOON (the blue dashed line), especially for a modest photon number. A recent numerical simulation shows that this improved sensitivity of the ECS can be maintained in the presence of the photon losses for $\bar{n} \lesssim 5$ [42]. However, the performance of the ECS with larger \bar{n} remains unclear.

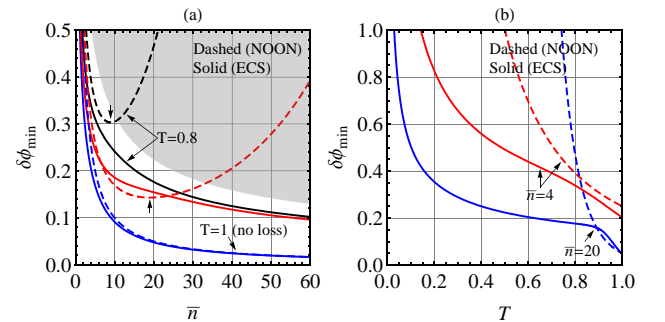


FIG. 1: (Color online) The ultimate precision $\delta\phi_{\min}$ against the number of photons \bar{n} or N and the transmission rate T (b) for the NOON (dashed) and the ECS (solid) states. In (a), $T = 1$ (blue lines), 0.9 (red lines), and 0.8 (black lines). Two arrows indicate $N_{\text{opt}} = -2/\ln T$ with $T = 0.8$ and 0.9 . In (b), $\bar{n} = 4$ (red lines) and 20 (blue lines). A crossover of $\delta\phi_{\min}$ between the ECS and the NOON states occurs for \bar{n} (or N) = 20 and $T \in (0.85, 1)$. Shaded area in (a): Region for the sensitivity worse than the shot-noise limit $1/\sqrt{\bar{n}}$.

III. QUANTUM FISHER INFORMATION AND ULTIMATE PRECISION OF ENTANGLED COHERENT STATE WITH PHOTON LOSSES

In this section, we present an exact analytical expression of the QFI F_Q and hence the ultimate precision $\delta\phi_{\min} = 1/\sqrt{F_Q}$ for the ECS in the presence of photon losses. This provides detailed information for the performance of the ECS in the quantum phase estimation, especially those at relatively large photon numbers, that are inaccessible from the previous numerical simulation. Firstly, we derive exact analytical expression of the quantum Fisher information for the input ECS based upon a general formula of the QFI. This formula decomposes the total QFI into three physically intuitive contributions. Next, we present the QFI of the NOON state. Finally, by comparing with the NOON state, we discuss the key features of the ECS and provides a simple physics picture.

The photon losses can be modeled by inserting two identical beam splitters $\hat{B}_{k,k'} = \exp[i(\theta/2)(\hat{a}_k^\dagger \hat{a}_k + h.c.)]$ that couples two sensor modes $k = 1, 2$ and two environment modes $k' = 1', 2'$ that are initially in the vacuum [35–44]. The action of beam splitters transforms the sensor mode \hat{a}_k^\dagger into a linear combination of \hat{a}_k^\dagger and $\hat{a}_{k'}^\dagger$: $\hat{B}_{k,k'} \hat{a}_k^\dagger \hat{B}_{k,k'}^{-1} = \sqrt{T} \hat{a}_k^\dagger + i\sqrt{R} \hat{a}_{k'}^\dagger$, where $T = \cos^2(\theta/2)$ and $R = 1 - T$ are transmission and absorption (loss) rates of the photons, respectively. More specially, $T = 1$ (i.e., $R = 0$) means no photon loss and $T = 0$ ($R = 1$) corresponds to complete photon loss. For the input ECS state, using $\hat{U}(\phi)|\alpha\rangle_2 = |\alpha e^{i\phi}\rangle_2$ and $\hat{B}_{k,k'}|\alpha\rangle_k = |\sqrt{T}\alpha\rangle_k |i\sqrt{R}\alpha\rangle_{k'}$, we obtain the outcome state

$$\begin{aligned} |\psi(\phi)\rangle &= N_\alpha \hat{B}_{1,1'} \hat{B}_{2,2'} \hat{U}(\phi) (|\alpha\rangle_1 + |\alpha\rangle_2) |0\rangle_{1'} |0\rangle_{2'} \\ &= N_\alpha (|\sqrt{T}\alpha\rangle_1 |E^{(1)}\rangle + |\sqrt{T}\alpha e^{i\phi}\rangle_2 |E^{(2)}\rangle), \end{aligned}$$

where the environment states are given by $|E^{(1)}\rangle \equiv |i\sqrt{R}\alpha\rangle_{1'} |0\rangle_{2'}$ and $|E^{(2)}\rangle \equiv |0\rangle_{1'} |i\sqrt{R}\alpha e^{i\phi}\rangle_{2'}$. Tracing over them, we obtain the reduced density matrix of the sensor modes

$$\begin{aligned} \hat{\rho} &= N_\alpha^2 \{ |\sqrt{T}\alpha\rangle_{11} \langle \sqrt{T}\alpha| + |\sqrt{T}\alpha e^{i\phi}\rangle_{22} \langle \sqrt{T}\alpha e^{i\phi}| \\ &\quad + \langle E^{(2)} | E^{(1)} \rangle (|\sqrt{T}\alpha\rangle_{12} \langle \sqrt{T}\alpha e^{i\phi}| + h.c.) \}, \end{aligned} \quad (4)$$

where $\langle E^{(2)} | E^{(1)} \rangle = \langle E^{(1)} | E^{(2)} \rangle = e^{-R|\alpha|^2}$. Compared with the lossless case (i.e., $T = 1$), the amplitudes in the sensor modes are reduced from $|\alpha|$ to $\sqrt{T}|\alpha|$. More importantly, the photon losses suppresses the off-diagonal coherence between the two sensor states by a factor $\langle E^{(2)} | E^{(1)} \rangle$. We will show below that this decoherence effect significantly degrades the estimation precision of the ECS.

Since $\hat{\rho}$ is a mixed state, to obtain the QFI one has to diagonalize it as $\hat{\rho} = \sum_m \lambda_m |\lambda_m\rangle \langle \lambda_m|$, where $\{|\lambda_m\rangle\}$ forms an orthonormalized and complete basis, with λ_m being the weight of $|\lambda_m\rangle$. According to the well-known formula [21–26], the QFI is given by

$$F_Q = \sum_{m,n} \frac{2}{\lambda_m + \lambda_n} |\langle \lambda_m | \hat{\rho}' | \lambda_n \rangle|^2, \quad (5)$$

where the prime denotes the derivation about ϕ , such as $\hat{\rho}' = \partial\hat{\rho}/\partial\phi$, $\lambda'_m = \partial\lambda_m/\partial\phi$, and $|\lambda'_m\rangle = \partial|\lambda_m\rangle/\partial\phi$. Typically, the dimension of entire Hilbert space and hence the basis $\{|\lambda_m\rangle\}$ is huge, but only a small subset has nonzero weights. Therefore, using the completeness and the ortho-normalization of $\{|\lambda_m\rangle\}$, we can express the QFI in terms of the subset $\{|\lambda_i\rangle\}$ with $\lambda_i \neq 0$ (see Appendix):

$$F_Q = \sum_i \frac{(\lambda'_i)^2}{\lambda_i} + \sum_i \lambda_i F_{Q,i} - \sum_{i \neq j} \frac{8\lambda_i \lambda_j}{\lambda_i + \lambda_j} |\langle \lambda'_i | \lambda_j \rangle|^2, \quad (6)$$

which contains three kinds of contributions. The first term is the classical Fisher information for the probability distribution $P(i|\phi) \equiv \lambda_i(\phi)$. The second term is a weighted average over the quantum Fisher information $F_{Q,i} = 4(\langle \lambda'_i | \lambda'_i \rangle - |\langle \lambda'_i | \lambda_i \rangle|^2)$ for each pure state in the subset $\{|\lambda_i(\phi)\rangle\}$ with $\lambda_i \neq 0$. The last term reduces the QFI and hence the estimation precision below the pure-state case. If the phase shift ϕ comes into the reduced density matrix $\hat{\rho}$ through the weights $\lambda_i(\phi)$ only, then the last two terms of Eq. (6) give vanishing contribution to the QFI. While for ϕ -independent weights, however, the first term vanishes.

Compared with Eq. (5) that relies on the complete basis, our formula Eq. (6), defined within a truncated Hilbert space, has the advantages of faster convergence and numerical stability, especially when the reduced density matrix $\hat{\rho}$ has some eigenvectors with extremely small but nonvanishing weights.

For the input ECS, we note that the reduced density matrix $\hat{\rho}$ only contains two sensor states $|\sqrt{T}\alpha\rangle_1$ and $|\sqrt{T}\alpha e^{i\phi}\rangle_2$ [see Eq. (4)]. This feature enables us to expand $\hat{\rho}$ in terms of two eigenvectors with nonzero eigenvalues (see Append. A),

$$\hat{\rho} = \lambda_+ |\lambda_+(\phi)\rangle \langle \lambda_+(\phi)| + \lambda_- |\lambda_-(\phi)\rangle \langle \lambda_-(\phi)|, \quad (7)$$

where the eigenvalues $\lambda_\pm = N_\alpha^2(1 \pm e^{-R|\alpha|^2})(1 \pm e^{-T|\alpha|^2})$ are ϕ -independent and obey $\lambda_- + \lambda_+ = 1$. The phase-dependent eigenvectors are given by

$$|\lambda_\pm(\phi)\rangle = \eta_\pm [|\pm\sqrt{T}\alpha\rangle_1 + |\sqrt{T}\alpha e^{i\phi}\rangle_2], \quad (8)$$

with the normalization factors $\eta_\pm = 1/\sqrt{2(1 \pm e^{-T|\alpha|^2})}$. It is easy to prove that $\langle \lambda_\pm | \lambda_\pm \rangle = 1$ and $\langle \lambda_+ | \lambda_- \rangle = \langle \lambda_+ | \hat{\rho} | \lambda_- \rangle = 0$. Using Eq. (6), we obtain exact analytical expression of the QFI (see Appendix. B):

$$F_Q = F_Q^{\text{cl}} + F_Q^{\text{HL}}, \quad (9)$$

where the classical term $F_Q^{\text{cl}} = 2\bar{n}T[1 + Tw(\bar{n}e^{-\bar{n}})]$, and the Heisenberg term

$$F_Q^{\text{HL}} = (\bar{n}T)^2 \left(\frac{e^{-2R|\alpha|^2} - e^{-2T|\alpha|^2}}{1 - e^{-2T|\alpha|^2}} \right). \quad (10)$$

In the absence of photon losses (i.e., $R = 0$ and $T = 1$), our result reduces to the lossless case, i.e., Eq. (3). Compared with it, we find that the photon losses leads to two effects on the QFI (and hence the estimation precision). Firstly, it trivially reduces the photon number from \bar{n} in the input state to $\bar{n}T$ in

the output state. Secondly, it exponentially suppresses the QFI from $F_Q^{\text{HL}} \sim (\bar{n}T)^2$ to the classical scaling $\sim 2\bar{n}T$ (see below).

For a comparison, we also employ Eq. (6) to derive the QFI for the NOON state $(|N\rangle_1 + |N\rangle_2)/\sqrt{2}$. It is easy to write down the reduced density matrix in a diagonal form:

$$\hat{\rho} = \sum_{n=0}^{N-1} \lambda_n (|n\rangle_{11} \langle n| + |n\rangle_{22} \langle n|) + T^N |\psi_{\text{NOON}}\rangle \langle \psi_{\text{NOON}}|, \quad (11)$$

where the first part is an incoherent mixture of Fock states $|n\rangle_1$ and $|n\rangle_2$ with ϕ -independent weights $\lambda_n = \binom{N}{n} T^n R^{N-n}/2$. The phase information is stored in the second part, $|\psi_{\text{NOON}}\rangle = (|N\rangle_1 + e^{iN\phi}|N\rangle_2)/\sqrt{2}$, which, for the lossless case, gives the QFI N^2 . Therefore, according to Eq. (6), the total QFI is equal to the QFI of $|\psi_{\text{NOON}}\rangle$ times its weight T^N , namely

$$F_{Q,\text{NOON}} = N^2 T^N, \quad (12)$$

in agreement with Ref. 35. With increasing photon number N , the ultimate precision $\delta\phi_{\text{min}} = T^{-N/2}/N$ shows a global minimum at $N_{\text{opt}} = -2/\ln T \approx 2/R$ (as $T = 1 - R \approx e^{-R}$ for small R), indicated by the arrows of Fig. 1(a).

In Fig. 1(a), we plot $\delta\phi_{\text{min}}$ of the ECS (the NOON) state as a function of number of photons \bar{n} (N) for the transmission rates $T = 0.8, 0.9$, and 1 (from top to bottom). Regardless of T , one can find that $\delta\phi_{\text{min}}$ of the input ECS decreases monotonically with the increase of \bar{n} . While for the NOON state, however, $\delta\phi_{\text{min}}$ reaches its minimum at N_{opt} and then grows rapidly. In Fig. 1(b), we show $\delta\phi_{\text{min}}$ against T for \bar{n} (N) = 4 and 20. It is interesting to note that a crossover of $\delta\phi_{\text{min}}$ between the ECS and the NOON states occurs for large \bar{n} and T (say, $T > 0.85$).

We now analyze the QFI under practical conditions: $T \sim 1$ ($R \sim 0$) and $|\alpha|^2 \gg 1$, for which $w(\bar{n}e^{-\bar{n}}) \approx 0$ and hence $|\alpha|^2 \approx \bar{n}$. In addition, the exponential term $e^{-2T|\alpha|^2}$ of Eq. (10) is negligible. As a result, the QFI reduces to

$$F_Q = F_Q^{\text{cl}} + F_Q^{\text{HL}} \approx 2\bar{n}T + (\bar{n}T)^2 e^{-2R\bar{n}}, \quad (13)$$

where the exponential term $e^{-2R\bar{n}} = |\langle E^{(2)}|E^{(1)}\rangle|^2$, quantifies the off-diagonal coherence of the sensor states. When the number of photons being lost $R\bar{n} = (1-T)\bar{n} \ll 1$, the Heisenberg term $F_Q^{\text{HL}} \approx (\bar{n}T)^2 e^{-2R\bar{n}}$ dominates and the ultimate precision obeys $\delta\phi_{\text{min}}^{\text{HL}} \approx e^{R\bar{n}}/(\bar{n}T)$. With the increase of $R\bar{n}$, the classical term $F_Q^{\text{cl}} \approx 2\bar{n}T$ becomes important. As $R\bar{n} \gg 1$, a complete decoherence of the two sensor states occurs due to $|\langle E^{(2)}|E^{(1)}\rangle|^2 \rightarrow 0$, leading to the completely mixed state

$$\hat{\rho} \approx \frac{1}{2} (|\sqrt{T}\alpha\rangle_{11} \langle \sqrt{T}\alpha| + |\sqrt{T}\alpha e^{i\phi}\rangle_{22} \langle \sqrt{T}\alpha e^{i\phi}|), \quad (14)$$

where the first term $|\sqrt{T}\alpha\rangle_{11} \langle \sqrt{T}\alpha|$ carries no phase information and hence $F_{Q,1} = 0$, and the ϕ -dependent second term $|\sqrt{T}\alpha e^{i\phi}\rangle_{22} \langle \sqrt{T}\alpha e^{i\phi}|$ produces the pure-state QFI $F_{Q,2} \approx 4\bar{n}T$. Therefore, according to Eq. (6), the total QFI of $\hat{\rho}$ reads $F_Q \approx \sum_i \lambda_i F_{Q,i} \approx 2\bar{n}T$, which in turn gives the classical scaling of the sensitivity $\delta\phi_{\text{min}} \approx \delta\phi_{\text{min}}^{\text{cl}} \approx 1/\sqrt{2\bar{n}T}$. In Fig. 2, we present the log-log plot of $\delta\phi_{\text{min}}$ for the loss rate $R = 0.1$ and 0.01. As shown by the red solid line, the simple formula

of Eq. (13) agrees quite well with the exact result (the solid circles). They both show a turning point at $\bar{n} \sim 1/R$. Indeed, the crossover of the quantum-classical transition takes place when the Heisenberg term F_Q^{HL} is comparable with the classical term F_Q^{cl} , i.e., $R\bar{n} \sim 1$.

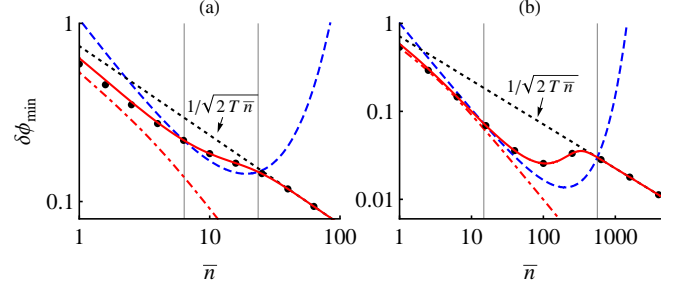


FIG. 2: (Color online) log-log plot of $\delta\phi_{\text{min}}$ for $T = 0.9$ (a) and $T = 0.99$ (b). Black dotted line: the classical limit $1/\sqrt{2\bar{n}T}$; Blue dashed line: $\delta\phi_{\text{min}}$ of the NOON state; Red solid line (circles): approximated (exact) $\delta\phi_{\text{min}}$ of the ECS; Red dot-dashed line: $\delta\phi_{\text{min}}$ of the ECS in the absence of photon losses (i.e., $T = 1$), given by Eq. (3). The two vertical lines at $\bar{n} = 6.4$ and 23.5 in (a) and $\bar{n} = 14.8$ and 561 in (b) show the crossover of $\delta\phi_{\text{min}}$ between the ECS and the NOON states.

For the ECS with large photon losses, i.e., $R\bar{n} \gg 1$, the ultimate precision $\delta\phi_{\text{min}}$ obeys the classical scaling $1/\sqrt{2\bar{n}T}$, which is conformed by Fig. 2. The precision of the NOON state is optimal at $\bar{n} = -2/\ln T \approx 2/R$ and then rapidly degrades below the classical limit [see the dashed lines, also Fig. 1(a)]. This is in sharp contrast to the ECS state. Qualitatively, different behaviors of the two states arises from the differently influences of photon losses:

1. For the ECS $\sim |\alpha\rangle_1 + |\alpha\rangle_2$, the off-diagonal coherence between the two sensor states $|\sqrt{T}\alpha\rangle_1$ and $|\sqrt{T}\alpha e^{i\phi}\rangle_2$ is exponentially suppressed by the photon losses, but the diagonal components of $\hat{\rho}$ still carries the phase information [see Eq. (14)], which contributes the QFI $F_Q \approx 2\bar{n}T$.
2. For the NOON state $\sim |N\rangle_1 + |N\rangle_2$, the phase information is stored only in the coherence part of $\hat{\rho}$ [see Eq. (11)], which decays with the photon losses as $T^N \approx e^{-RN}$ for small R . When the lost photon number $RN \gg 1$, the information about the phase shift ϕ is completely eliminated.

From Fig. 1, we have observed the crossover of $\delta\phi_{\text{min}}$ between the ECS and the NOON states, which can be understood by simply comparing the QFIs for the two states. Without the photon losses, the ultimate precision of the ECS always surpass those of the NOON states because $F_Q = F_Q^{\text{cl}} + F_Q^{\text{HL}} > F_{Q,\text{NOON}}$ (as $F_Q^{\text{HL}} = F_{Q,\text{NOON}} = \bar{n}^2$). In the presence of moderate photon losses, the Heisenberg term $F_Q^{\text{HL}} \approx (\bar{n}T)^2 e^{-2R\bar{n}}$ decays more quickly than that of the NOON state $F_{Q,\text{NOON}} \approx \bar{n}^2 e^{-R\bar{n}}$. This makes it possible for the NOON state to outperform the ECS when the quantum contribution F_Q^{HL} dominates the classical contribution F_Q^{cl} . From Fig. 2, one can

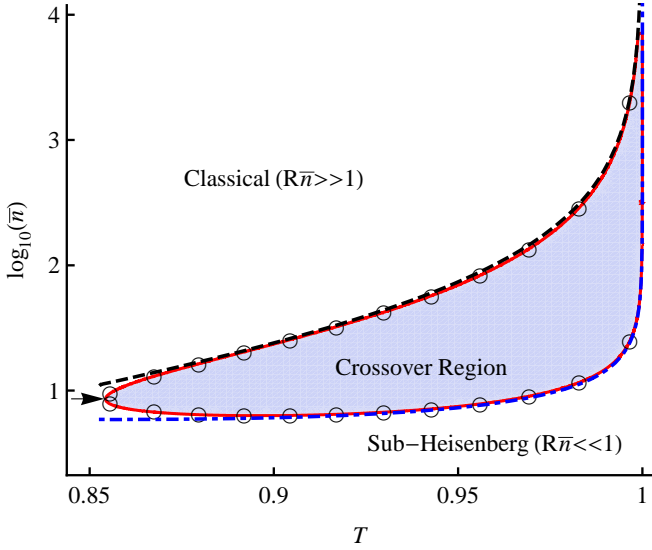


FIG. 3: (Color online) The crossover region in which $\delta\phi_{\min}$ of the NOON state is preferable. Red solid line: $\bar{n}T^{\bar{n}-1} = 2 + \bar{n}Te^{-2R\bar{n}}$ for $R = 1 - T$ and $T \in (0.85, 1)$; Black dashed and blue dot-dashed lines: $\bar{n}_u \approx 3.2T^6/R^{1.15}$ and $\bar{n}_l \approx 1.4T^{-3}/R^{0.5}$, fitting very well with the boundary of the crossover region (Open circles). The critical point of the crossover: $(T, \bar{n}) = (0.854, 8.58)$, as indicated by the arrow.

find that the NOON states with $\bar{n} \in (6.4, 23.5)$ for $R = 0.1$ and $\bar{n} \in (14.8, 561)$ for $R = 0.01$ are preferable, within the vertical lines of Fig. 2.

In general, the crossover condition can be obtained by equating Eq. (13) and Eq. (12). This gives a transcendental equation: $\bar{n}T^{\bar{n}-1} \approx 2 + \bar{n}Te^{-2R\bar{n}}$, as illuminated by the red solid curve in Fig. 3. It shows that the NOON states outperforms the ECS inside the crossover region, while the ECS prevails outside. The upper and the lower boundaries of the region are well fitted by $\bar{n}_u \approx 3.2T^6/R^{1.15}$ (the black dashed line) and $\bar{n}_l \approx 1.4T^{-3}/R^{1/2}$ (the blue dash-dotted line), respectively. The upper boundary corresponds to $F_{Q,\text{NOON}} \approx F_{Q,\text{ECS}}^{\text{cl}}$. As shown in Fig. 3, we find that the crossover of $\delta\phi_{\min}$ between the ECS and the NOON states takes place for $T \in (0.854, 1)$. For such a relatively low loss rate ($0 < R < 0.15$), the precision of the NOON state could surpass that of the ECS over a wider range of \bar{n} until the classical term $F_{Q,\text{ECS}}^{\text{cl}}$ begins to dominate. However, the NOON states with $\bar{n} > \bar{n}_u$ ceases to be optimal and its precision gets even worse than the classical limit [35]. From Fig. 3, we also note that no crossover occurs for $T \lesssim 0.854$ and the ultimate precision of the ECS is always better than that of the NOON state [see also the black lines of Fig. 1(a)].

IV. CONCLUSION

By considering a superposition of NOON states as “input” of a lossless optical interferometer, we have shown that the quantum Fisher information $F_Q \geq \bar{n}^2$ and therefore the ultimate precision of phase sensitivity can be better than the Heisenberg limit.

As a special case of the superposed state, an entangled co-

herent state $\propto |\alpha, 0\rangle_{1,2} + |0, \alpha\rangle_{1,2}$ has been investigated. Exact result of the quantum Fisher information is obtained to investigate the role of photon losses on the lower bound of phase sensitivity $\delta\phi_{\min}$. Without the photon losses, i.e., the absorption rate $R = 0$ and the transmission rate $T = 1$, we confirm that the input ECS always outperform the NOON state [42]. In the presence of photon losses, the transition of $\delta\phi_{\min}$ from the Heisenberg scaling to the classical limit occurs due to the loss-induced quantum decoherence between the sensor states. The quantum-classical transition depends upon the number of photons being lost $R\bar{n}$, but rather the total photon number \bar{n} or the lose rate R alone. For a given transmission rate $T \in (0.85, 1)$, we also find that there exists a crossover of $\delta\phi_{\min}$ between the ECS and the NOON states. The NOON state is preferable in the crossover region, i.e., $\bar{n}T^{\bar{n}-1} \geq 2 + \bar{n}Te^{-2R\bar{n}}$. For $R\bar{n} \gg 1$, however, the precision of the NOON state degrades below the classical limit; While for the ECS state, $\delta\phi_{\min}$ obeys the classical limit $1/\sqrt{2T\bar{n}}$, better than that of the NOON state.

Acknowledgments

We thank Professor D. L. Zhou and Professor J. P. Dowling for helpful discussions. This work is supported by Natural Science Foundation of China (NSFC, Contract Nos. 11174028 and 11274036), the Fundamental Research Funds for the Central Universities (Contract No. 2011JBZ013), and the Program for New Century Excellent Talents in University (Contract No. NCET-11-0564). X.W.L is partially supported by National Innovation Experiment Program for University Students.

Appendix A: Eigenvalues and Eigenvectors of the reduced density matrix

We present a general method to diagonalize the reduced density matrix likes Eq. (4). The eigenvector of $\hat{\rho}$ can be spanned as $|\lambda(\phi)\rangle = \sum_j c_j |\Phi_j\rangle$, where the states $|\Phi_j\rangle$ are not necessary orthogonal. Using the eigenvalue equation: $\hat{\rho}|\lambda(\phi)\rangle = \lambda|\lambda(\phi)\rangle$, or equivalently $\sum_j \langle \Phi_i | \hat{\rho} | \Phi_j \rangle c_j = \lambda \sum_j \langle \Phi_i | \Phi_j \rangle c_j$, we can determine the eigenvalue λ and the amplitudes c_j . It is convenient to write down the eigenvalue equation in a matrix form: $\boldsymbol{\rho}\mathbf{c} = \lambda\mathbf{A}\mathbf{c}$, where the elements of $\boldsymbol{\rho}$ and \mathbf{A} are $\rho_{ij} = \langle \Phi_i | \hat{\rho} | \Phi_j \rangle$ and $A_{ij} = \langle \Phi_i | \Phi_j \rangle$, and $\mathbf{c} = (c_1, c_2, \dots)^T$. Multiplying the inverse matrix \mathbf{A}^{-1} on the left, we can rewrite the eigenvalue equation as

$$\tilde{\boldsymbol{\rho}}\mathbf{c} \equiv \mathbf{A}^{-1}\boldsymbol{\rho}\mathbf{c} = \lambda\mathbf{c}, \quad (\text{A1})$$

where $\tilde{\boldsymbol{\rho}} = \mathbf{A}^{-1}\boldsymbol{\rho}$.

Using the above formula, we now diagonalize the reduced density operator of Eq. (4). Firstly, we expand the eigenvectors as $|\lambda(\phi)\rangle = c_1|\Phi_1\rangle + c_2|\Phi_2\rangle$, where $|\Phi_1\rangle = |\sqrt{T}\alpha\rangle_1 = |\sqrt{T}\alpha\rangle_1|0\rangle_2$ and $|\Phi_2\rangle = |\sqrt{T}\alpha e^{i\phi}\rangle_2 = |0\rangle_1|\sqrt{T}\alpha e^{i\phi}\rangle_2$. It is easy to obtain the matrix

$$\tilde{\boldsymbol{\rho}} = \mathcal{N}_\alpha^2 \begin{pmatrix} 1 + e^{-|\alpha|^2} & e^{-T|\alpha|^2} + e^{-R|\alpha|^2} \\ e^{-T|\alpha|^2} + e^{-R|\alpha|^2} & 1 + e^{-|\alpha|^2} \end{pmatrix},$$

where T ($R = 1 - T$) are the transmission (absorption) rate of the photons and $\mathcal{N}_\alpha^2 = 1/[2(1 + e^{-|\alpha|^2})]$. Next, from the equation $|\lambda\mathbf{I} - \tilde{\rho}| = 0$, we obtain the eigenvalues

$$\lambda_\pm = \mathcal{N}_\alpha^2 \left[(1 + e^{-|\alpha|^2}) \pm (e^{-T|\alpha|^2} + e^{-R|\alpha|^2}) \right], \quad (\text{A2})$$

which obeys $\lambda_- + \lambda_+ = 1$. Substituting λ_\pm into Eq. (A1), or $(\lambda\mathbf{I} - \tilde{\rho})\mathbf{c} = 0$, we further obtain the amplitudes $c_1 = \pm c_2$, i.e., the eigenvectors $|\lambda_\pm(\phi)\rangle \propto (\pm|\sqrt{T}\alpha\rangle_1 + |\sqrt{T}\alpha e^{i\phi}\rangle_2)$, as Eq. (8).

Appendix B: Derivations of the quantum Fisher information

Firstly, we derive the general expression of the QFI [i.e., Eq. (6)]. For a mixed state $\hat{\rho} = \sum_m \lambda_m |\lambda_m\rangle\langle\lambda_m|$, the QFI is given by the well-known formula of Eq. (5), where the eigenvectors of the reduced density matrix $\{|\lambda_m\rangle\}$ span an orthonormalized and complete basis. In general, the dimension of the entire Hilbert space is huge. However, there exists a much smaller subset $\{|\lambda_i\rangle\}$ with nonzero weights λ_i . It is convenient to express the QFI in terms of this subset only. For this purpose, we divide the complete basis $\{|\lambda_m\rangle\}$ into two subsets: $\{|\lambda_i\rangle\}$ and $\{|\lambda_{\bar{i}}\rangle\}$, with $\lambda_i \neq 0$ and $\lambda_{\bar{i}} = 0$, respectively. Using the completeness relation $\sum_{\bar{i}} |\lambda_{\bar{i}}\rangle\langle\lambda_{\bar{i}}| = 1 - \sum_i |\lambda_i\rangle\langle\lambda_i|$, Eq. (5) can be rewritten as

$$F_Q = \sum_i \frac{2\langle\lambda_i|(\hat{\rho}')^2|\lambda_i\rangle}{\lambda_i} + \sum_j \frac{2\langle\lambda_j|(\hat{\rho}')^2|\lambda_j\rangle}{\lambda_j} + \sum_{i,j} 2 \left(\frac{1}{\lambda_i + \lambda_j} - \frac{1}{\lambda_i} - \frac{1}{\lambda_j} \right) |\langle\lambda_i|\hat{\rho}'|\lambda_j\rangle|^2, \quad (\text{B1})$$

where only the subset $\{|\lambda_i\rangle\}$ with $\lambda_i \neq 0$ is involved. Since $\{|\lambda_i\rangle\}$ are ortho-normalized, i.e., $\langle\lambda_i|\lambda_j\rangle = \delta_{i,j}$, we have $\langle\lambda_i|\lambda'_j\rangle + \langle\lambda'_i|\lambda_j\rangle = 0$, and hence

$$\begin{aligned} \langle\lambda_i|(\hat{\rho}')^2|\lambda_i\rangle &= (\lambda'_i)^2 + \lambda_i^2 \langle\lambda'_i|\lambda'_i\rangle \\ &\quad + \sum_{\bar{i}} (\lambda_{\bar{i}}^2 - 2\lambda_i\lambda_{\bar{i}}) |\langle\lambda'_i|\lambda_{\bar{i}}\rangle|^2, \\ |\langle\lambda_i|\hat{\rho}'|\lambda_j\rangle|^2 &= (\lambda'_i)^2 \delta_{i,j} + (\lambda_i - \lambda_j)^2 |\langle\lambda'_i|\lambda_j\rangle|^2. \end{aligned}$$

Substituting them into Eq. (B1), and using $|\langle\lambda'_j|\lambda_i\rangle|^2 = |\langle\lambda'_i|\lambda_j\rangle|^2$, we obtain the general formula of the QFI as main text of Eq. (6).

Now we apply the general formula to calculate the QFI of the ECS state. Since the eigenvalues of the reduced density

matrix λ_\pm are phase-independent, the first term of Eq. (6) vanishes. From Eq. (8), it is easy to obtain the derivation of the eigenvectors

$$|\lambda'_\pm\rangle = \eta_\pm \frac{\partial}{\partial\phi} |\sqrt{T}\alpha e^{i\phi}\rangle_2 = \eta_\pm \sum_{n=0}^{\infty} i n d_n(\alpha \sqrt{T} e^{i\phi}) |n\rangle_2, \quad (\text{B2})$$

where the normalization factors $\eta_\pm = 1/\sqrt{2(1 \pm e^{-T|\alpha|^2})}$ and the probability amplitudes of coherent state $d_n(\alpha) \equiv \langle n|\alpha\rangle = \alpha^n e^{-\frac{1}{2}|\alpha|^2}/\sqrt{n!}$, which satisfy $\sum_n |d_n(\alpha)|^2 = 1$ and

$$\sum_{n=0}^{+\infty} n |d_n(\alpha)|^2 = |\alpha|^2, \quad \sum_{n=0}^{+\infty} n^2 |d_n(\alpha)|^2 = |\alpha|^2(1 + |\alpha|^2).$$

Therefore, combining Eq. (8) and Eq. (B2), we obtain

$$\langle\lambda_\pm|\lambda'_\pm\rangle = \eta_\pm^2 \sum_{n=0}^{\infty} i n |d_n(\alpha e^{i\phi} \sqrt{T})|^2 = i \eta_\pm^2 |\alpha|^2 T, \quad (\text{B3})$$

and similarly, $\langle\lambda_\mp|\lambda'_\mp\rangle = i \eta_\mp \eta_\pm |\alpha|^2 T$, as well as $\langle\lambda'_\pm|\lambda'_\pm\rangle = \eta_\pm^2 |\alpha|^2 T(1 + |\alpha|^2 T)$. These results enable us to calculate the remaining terms of Eq. (6):

$$\begin{aligned} \sum_{i=\pm} \lambda_i F_{Q,i} &= 4\lambda_+ \eta_+^2 |\alpha|^2 T(1 + |\alpha|^2 T - \eta_+^2 |\alpha|^2 T) \\ &\quad + 4\lambda_- \eta_-^2 |\alpha|^2 T(1 + |\alpha|^2 T - \eta_-^2 |\alpha|^2 T), \quad (\text{B4}) \end{aligned}$$

and

$$\sum_{i=\pm, j=\mp} \frac{8\lambda_i \lambda_j}{\lambda_i + \lambda_j} |\langle\lambda'_i|\lambda_j\rangle|^2 = 16\lambda_+ \lambda_- \eta_+^2 \eta_-^2 |\alpha|^4 T^2, \quad (\text{B5})$$

due to $\lambda_+ + \lambda_- = 1$. Finally, we get the exact result of the QFI for the input ECS:

$$F_Q = 4\mathcal{N}_\alpha^2 |\alpha|^2 T \left[1 + |\alpha|^2 T - \mathcal{N}_\alpha^2 |\alpha|^2 T \left(1 + \frac{1 - e^{-2R|\alpha|^2}}{1 - e^{-2T|\alpha|^2}} \right) \right],$$

where we have used the relations: $\lambda_+ \eta_+^2 + \lambda_- \eta_-^2 = \mathcal{N}_\alpha^2$ and $4\lambda_+ \lambda_- \eta_+^2 \eta_-^2 = \mathcal{N}_\alpha^4 [1 - e^{-2R|\alpha|^2}]$, as well as

$$\lambda_+ \eta_+^4 + \lambda_- \eta_-^4 = \frac{\mathcal{N}_\alpha^2}{2} \frac{1 - e^{-|\alpha|^2}}{1 - e^{-2T|\alpha|^2}}.$$

Using $\bar{n} = 2\mathcal{N}_\alpha^2 |\alpha|^2$ and hence $|\alpha|^2 = \bar{n} + w(\bar{n} e^{-\bar{n}})$, the QFI can be further simplified as Eq. (9).

-
- [1] C. M. Caves, Phys. Rev. D **23**, 1693 (1981).
[2] B. Yurke, S. L. McCall, and J. R. Klauder, Phys. Rev. A **33**, 4033 (1986).
[3] M. J. Holland, and K. Burnett, Phys. Rev. Lett. **71**, 1355 (1993).
[4] D. J. Wineland, J. J. Bollinger, W. M. Itano, and D. J. Heinzen, Phys. Rev. A **50**, 67 (1994).
[5] D. Leibfried, M. D. Barrett, T. Schaetz, J. Britton, J. Chiaverini, W. M. Itano, J. D. Jost, C. Langer, and D. J. Wineland, Science **304**, 1476 (2004).
[6] M. W. Mitchell, J. S. Lundeen, and A. M. Steinberg, Nature **429**, 161 (2004).
[7] V. Giovannetti, S. Lloyd, and L. Maccone, Nature Photonics **5**, 222 (2011); *ibid.*, Science **306**, 1330 (2004).
[8] A. Luis, Phys. Lett. A **329**, 8 (2004).
[9] A. M. Rey, L. Jiang, and M. D. Lukin, Phys. Rev. A **76**, 053617 (2007).

- [10] S. Boixo, A. Datta, S. T. Flammia, A. Shaji, E. Bagan, and C. M. Caves, *Phys. Rev. A* **77**, 012317 (2008).
- [11] S. Choi, and B. Sundaram, *Phys. Rev. A* **77**, 053613 (2008).
- [12] M. J. Woolley, G. J. Milburn, and C. M. Caves, *New J. Phys.* **10**, 125018 (2008).
- [13] Y. C. Liu, G. R. Jin, and L. You, *Phys. Rev. A* **82**, 045601 (2010); G. R. Jin, Y. C. Liu, and L. You, *Front. Phys.* **6**, 251 (2011).
- [14] J. J. Bollinger, W. M. Itano, D. J. Wineland, and D. J. Heinzen, *Phys. Rev. A* **54**, R4649 (1996).
- [15] T. Kim, O. Pfister, M. J. Holland, J. Noh, and J. L. Hall, *Phys. Rev. A* **57**, 4004 (1998).
- [16] R. A. Campos, C. C. Gerry, and A. Benmoussa, *Phys. Rev. A* **68**, 023810 (2003).
- [17] J. P. Dowling, *Contemp. Phys.* **49**, 125 (2008); P. M. Anisimov, G. M. Raterman, A. Chiruvelli, W. N. Plick, S. D. Huver, H. Lee, and J. P. Dowling, *Phys. Rev. Lett.* **104**, 103602 (2010).
- [18] B. Lücke, M. Scherer, J. Kruse, L. Pezzé, F. Deuretzbacher, P. Hyllus, O. Topic, J. Peise, W. Ertmer, J. Arlt, L. Santos, A. Smerzi, and C. Klempt, *Science* **334**, 773 (2011).
- [19] C. W. Helstrom, *Quantum Detection and Estimation Theory* (Academic Press, New York, 1976).
- [20] A. S. Holevo, *Probabilistic and Statistical Aspect of Quantum Theory* (North-Holland Press, Pisa 1982).
- [21] S. L. Braunstein and C. M. Caves, *Phys. Rev. Lett.* **72**, 3439 (1994).
- [22] S. L. Braunstein, C. M. Caves, and G. J. Milburn, *Ann. Phys. (N.Y.)* **247**, 135 (1996).
- [23] L. Pezzé and A. Smerzi, *Phys. Rev. Lett.* **102**, 100401 (2009).
- [24] Z. Sun, J. Ma, X. M. Lu, and X. Wang, *Phys. Rev. A* **82**, 022306 (2010).
- [25] M. Kacprowicz, R. Demkowicz-Dobrzański, W. Wasilewski, K. Banaszek, and I. A. Walmsley, *Nature Photonics* **4**, 357 (2010).
- [26] W. Zhong, Z. Sun, J. Ma, X. Wang, and F. Nori, *Phys. Rev. A* **87**, 022337 (2013).
- [27] M. G. Genoni, S. Olivares, and M. G. A. Paris, *Phys. Rev. Lett.* **106**, 153603 (2011); M. G. Genoni, S. Olivares, D. Brivio, S. Cialdi, D. Cipriani, A. Santamato, S. Vezzoli, and M. G. A. Paris, *Phys. Rev. A* **85**, 043817 (2012).
- [28] B. M. Escher, L. Davidovich, N. Zagury, and R. L. de Matos Filho, *Phys. Rev. Lett.* **109**, 190404 (2012).
- [29] J. Ma, Y. X. Huang, X. Wang, and C. P. Sun, *Phys. Rev. A* **84**, 022302 (2011).
- [30] M. D. Lang, and C. M. Caves, arXiv:1306.2677 (2013).
- [31] C. C. Gerry, *Phys. Rev. A* **61**, 043811 (2000).
- [32] A. N. Boto, P. Kok, D. S. Abrams, S. L. Braunstein, C. P. Williams, and J. P. Dowling, *Phys. Rev. Lett.* **85**, 2733 (2000).
- [33] C. C. Gerry, A. Benmoussa, and R. A. Campos, *Phys. Rev. A* **66**, 013804 (2002).
- [34] H. Lee, P. Kok, and J. P. Dowling, *J. Mod. Opt.* **49**, 2325 (2002).
- [35] U. Dorner, R. Demkowicz-Dobrzański, B. J. Smith, J. S. Lundeen, W. Wasilewski, K. Banaszek, and I. A. Walmsley, *Phys. Rev. Lett.* **102**, 040403 (2009); R. Demkowicz-Dobrzański, U. Dorner, B. J. Smith, J. S. Lundeen, W. Wasilewski, K. Banaszek, and I. A. Walmsley, *Phys. Rev. A* **80**, 013825 (2009).
- [36] B. M. Escher, R. L. de Matos Filho, and L. Davidovich, *Nature Phys.* **7**, 406 (2011); B. M. Escher, R. L. de Matos Filho, and L. Davidovich, *Brazil. J. Phys.* **41**, 220 (2011).
- [37] R. Demkowicz-Dobrzański, J. Kolodynski, and M. Guta, *Nature Commun.* **3**, 1063 (2012).
- [38] S. J. van Enk, *Phys. Rev. A* **72**, 022308 (2005).
- [39] T.-W. Lee, S. D. Huver, H. Lee, L. Kaplan, S. B. McCracken, C. J. Min, D. B. Uskov, C. F. Wildfeuer, G. Veronis, and J. P. Dowling, *Phys. Rev. A* **80**, 063803 (2009).
- [40] J. J. Cooper, D. W. Hallwood, and J. A. Dunningham, *Phys. Rev. A* **81**, 043624 (2010).
- [41] S. Knysh, V. N. Smelyanskiy, and G. A. Durkin, *Phys. Rev. A* **83**, 021804(R) (2011).
- [42] J. Joo, W. J. Munro, and T. P. Spiller, *Phys. Rev. Lett.* **107**, 083601 (2011); J. Joo, K. Park, H. Jeong, W. J. Munro, K. Nemoto, and T. P. Spiller, *Phys. Rev. A* **86**, 043828 (2012).
- [43] M. Jarzyna and R. Demkowicz-Dobrzański, *Phys. Rev. A* **85**, 011801(R) (2012).
- [44] J. J. Cooper, D. W. Hallwood, J. A. Dunningham, and J. Brand, *Phys. Rev. Lett.* **108**, 130402 (2012).
- [45] C. C. Gerry and P. L. Knight, *Introductory Quantum Optics* (Cambridge University Press, Cambridge, England, 2005).
- [46] T. Ono and H. F. Hofmann, *Phys. Rev. A* **81**, 033819 (2010); H. F. Hofmann, *ibid.* **79**, 033822 (2009); H. F. Hofmann and T. Ono, *ibid.* **76**, 031806(R) (2007); A. Luis, *ibid.* **64**, 054102 (2001).
- [47] A. Ourjoumtsev, R. Tualle-Brouiri, J. Laurat, P. Grangier, *Science* **312**, 83 (2006); A. Ourjoumtsev, H. Jeong, R. Tualle-Brouiri, P. Grangier, *Nature* **448**, 784 (2007); H. Takahashi, K. Wakui, S. Suzuki, M. Takeoka, K. Hayasaka, A. Furusawa, and M. Sasaki, *Phys. Rev. Lett.* **101**, 233605 (2008); T. Gerrits, S. Glancy, T. S. Clement, B. Calkins, A. E. Lita, A. J. Miller, A. L. Migdall, S. W. Nam, R. P. Mirin, and E. Knill, *Phys. Rev. A* **82**, 031802(R) (2010).